

SEGREGATION AND MIXING OF GRANULAR MATERIAL IN INDUSTRIAL PROCESSES

TOM A.H. SIMONS^{*1,2}, M. DEL MAR COMBARROS-GARCIA^{1,2}, PRASHANT GUPTA³, UGUR TÜZÜN⁴, STEFAN ZIGAN⁵, JIN SUN³, MARTIN SCHILLING¹, SVEN BENSMANN¹, HARALD ZETZENER², HERMANN J. FEISE¹, ARNO KWADE², FRANK KLEINE-JÄGER¹, JIN Y. OOI³

¹ BASF SE, Chemical and Process Engineering, 67056 Ludwigshafen, Germany, e-mail: tom.a.simons@basf.com

² TU Braunschweig, Institute for Particle Technology, 38104 Braunschweig, Germany, e-mail: m.combarros-garcia@tu-bs.de

³ University of Edinburgh, Institute for Infrastructure and Environment, EH9 3JY, Edinburgh, UK, e-mail: p.gupta@ed.ac.uk

⁴ University of Oxford, Department of Engineering Science, Oxford, UK

⁵ University of Greenwich, Department of Engineering Systems, Chatham, UK

Keywords: Segregation, mixing, DEM, PARDEM, fluidized beds, silos, ribbon-blade mixers.

Abstract. Within the EU-funded PARDEM network mixing and segregation are studied in silos and heaps, agitated mixers and fluidized beds. A method is presented with which mixing and segregation can be characterized, adapted for quasi-static to dynamic systems and applied at the global system level as well as at the local level. This paper attempts to give an overview of the applicability of this analysis by providing three instances, being chute flow representing flow down a heap, agitated mixing and fluidization, in which the method is applied.

1. INTRODUCTION

The optimization of granular mixing performance as well as a sound understanding of the physical backgrounds of segregation of granular material is of considerable interest to both scientific and industrial communities. Better in-depth understanding of mixing and segregation behavior may well lead to reliable predictions of these phenomena in several unit operations in the near future. This opportunity may be offered by simulations with the Discrete Element Method (DEM) saving time and investments for experimental work, although it would not exclude experiments required for validation of the model.

These DEM results can then be used for a study to characterize extent, rate and propensity of mixing and segregation. The extent of segregation or mixing has been expressed in literature, through indices obtained from statistical analysis of fractions of the mixture's

constituents. This has been done over the last decades experimentally by intrusive methods such as sampling [1-6], and non-intrusive methods such as image analysis, including particle image velocimetry (PIV) [7-10], digital image analysis [11] and positron emission particle tracking (PEPT) [12-15], and by simulation [15-18]. Although this characterization is rather established, no standard for the mixing or segregation index has been defined, but is adapted to the mixing or segregation problem under investigation. An overview for mixing and segregation indices may be found in [1,6,19,20].

The rate of mixing or segregation can be interpreted as the change in mixedness per time unit throughout the mixture; propensity can be expressed as the tendency towards segregation or mixing at a local level within the system. The rate and propensity of mixing and segregation can be studied, based on work by Baxter et al. [21] and Christakis et al. [22-24], in which several causes of mixing and segregation and processing these effects into a continuum model were addressed.

Segregation and mixing mechanisms in granular flows can be identified as percolation (gravity driven segregation), kinetic sieving (strain-induced segregation), and diffusion effects (movement of particles along a concentration gradient), the latter being in fact mixing and working against the segregation effects [21]. There are both experimental and simulation routes to establish the magnitudes of the three source terms due to the three different segregation mechanisms. The contributions are assumed to be additive with independent superimposition. The model can be readily extended mathematically to systems comprising of sink terms such as simultaneous agglomeration and segregation or simultaneous attrition/degradation and segregation [23]. The influence of the interstitial fluid drag is incorporated as an additional term to shear induced segregation in cases where fluid-particle interactions are significant [25]. Examples in dense granular flows were given and their model was also applied to instances by Zigan et al. [26] in silos in which solid-air flow interaction plays a role.

In addition to the experimental route described above, for propensity and rate of segregation/mixing, the analysis presented below illustrates how the relevant transport (percolation), convection (shear) and concentration dependent diffusion coefficients can be calculated also directly from the DEM simulation results. Coefficients calculated would be useful to predict prevalent segregation mechanism by comparing the relative magnitudes, e.g. kinetic sieving coefficients were found to be two magnitudes greater than the diffusion coefficients for core hopper silo discharge. The percolation mechanism was found to be much weaker in this case [22].

For established analytical theory, definition of transport coefficients is established through linear response theory, i.e. response of a system to a perturbation [27,28]. In granular particle flow, e.g. fluidized beds, perturbations could be due to particle surface irregularities (asperity) or due to fluctuations of local fluid velocity field [29]. Transport mechanisms esp. diffusion for granular flow has been previously studied for non-cohesive [30,31], and cohesive grains [29]. Under assumption of steady state and thermo-dynamical equilibrium, a parallel was drawn between fluctuating particle velocity components and random Brownian motion of molecules in a dense gas [29,32].

The present work will attempt to arrive at the definition of a new composite index for segregation by summing the contributions of the percolation, kinetic and diffusion mechanisms described in detail below. As the relative contributions to the composite index will be different in the three industrial process applications modeled in the current study, the approach will allow the model user to distinguish the most prevalent mechanism in defining the segregation/mixing index rather than using an entirely empirical value obtained from accumulated data on segregated/mixed samples during the model experiments. The latter has been the approach to date in defining purely empirical segregation indices.

2. METHODOLOGY

2.1 Simulation models

DEM simulations of chute flow in the QPM tester (see section 3.1), a model silo and a ribbon blade mixer were conducted with LIGGGHTS [33]. DEM-CFD simulations of the fluidized bed were carried out using LammPSFOAM [34]. DEM equations were used as described in literature.

As developed by Cundall and Strack [35], particle motion can be described by Newtonian equations in a Lagrangian approach. These equations are then integrated numerically for particle positions and velocities when subject to total forces typical to the system [35]. These total forces, apart from gravity, consist of contact forces only for the QPM tester, the model silo and the ribbon blade mixer. These contact forces are calculated based on the contact model describing the interaction between particles. Linear and non-linear spring-dashpot models are described in the literature [35,36]. For the example cases presented here, using LIGGGHTS, the non-linear Hertz-Mindlin model was used, the force varying with the 3/2 power of the displacement [36], extended with a rolling friction model by Ai et al. [37], but without taking into account cohesion.

For gas-solid flows, a gas-particle interaction term and a cohesion term are added up to the contact forces. The gas-particle interaction term comprises of a drag model term, a buoyancy term arising due to pressure gradient across the particle and the macroscopic variations in the fluid stress tensor [38]. The cohesion force is modelled as Van der Waals-type force [39].

DEM equations are coupled with gas flows, modelled in a Eulerian framework, volume averaged Navier-Stokes were used as presented in [40,41]. The interphase momentum exchange can be modelled in terms of drag force, in the present paper the drag model as proposed by Beetstra et al. was used [42].

2.2 Calculation of mixing and segregation indices

Experimental results of chute flow and ribbon blade mixing were evaluated by calculation of an overall mixing index. In this work, the mixing index as defined by Lacey was used [1]. This mixing index defines the extent of mixing or segregation as a ratio of the state of mixing currently achieved to the maximum achievable state of mixing, being perfect random mixing (ideal stochastic mixture). The advantage of this index over some other indices is that it can

assume values for mixing homogeneity between 0 and 1; 0 being the completely segregated state and 1 being the ideal stochastic mixture.

2.3 Methodology for analysis of mixing/segregation

Continuum equations for mass and momentum can be written for an N species system [24]. In absence of sinks and sources, the volume fraction of an individual component f_i can be obtained by transport equations.

$$\frac{\partial f_i}{\partial t} + \nabla(f_i \vec{u}_b + \vec{J}_{segi}) = 0 \quad (1)$$

where u_b is the bulk velocity vector, f_i is the volume fraction of the type i and J_{segi} is a drift flux which dictates the motion of the individual species in the bulk and determines the segregation of the mixture. This term can be expressed splitting it in the different velocities corresponding to the different mechanisms found, being diffusion (v_{Di}), shear-induced segregation (v_{Si}) and gravity-driven percolation (v_{Pi}), as described by Christakis et al. [24] and shown in Equation 2.

$$J_{segi} = f_i(v_{Di} + v_{Si} + v_{Pi}) \quad (2)$$

A description of the three terms representing the segregation mechanisms is provided by Christakis et al (2002) [24].

3. EXPERIMENTAL AND SIMULATION SETUP

3.1 QPM tester

Segregation studies were performed with the QPM (quality in particulate manufacturing) segregation tester developed by the University of Greenwich [43]. The tester is used to quantify the intensity and distribution of segregation occurring in a bed of bulk solids. It isolates the mechanism of rolling segregation in a heap, generally found to be the principal cause of segregation in the charge and discharge of storage vessels with free-flowing particles. The tester consists of a cubic mixer and an inclined plane. The feed system allows the tester to be charged with a stream of particles uniformly distributed both along and across the feed stream. The mixture falls into a one-sided plane flow test section where it forms an angle of repose and, hence, segregates.

The material of each section can then be separated and analyzed as desired to measure the fraction of each material in this mixture. The same approach was used for the DEM simulations. From these DEM simulations, as already outlined in the introduction, the transport coefficient can then be calculated. The procedure is the same as followed by Christakis et al. [22,24].

3.2 Model silo filling and discharge

With the aim of validating the transport coefficients and the continuum model established, experiments in a larger scale have been performed. The bulk solids are placed initially on a

model silo mixing two materials. The materials used are glass beads of two different sizes with different colors allowing the measuring of the concentration profiles. The particle properties, bulk properties and the parameters used in the DEM Simulations are shown in Tables 1 and 2. The DEM parameters were calibrated by comparing the macroscopic responses of standard experiments of bulk materials and its simulations as reported in Combarros et al. [44].

Table 1: Material properties: model silo

| Property | Black glass beads | Silver glass beads |
|---------------------------------------|-------------------|--------------------|
| Shape | Spherical | Spherical |
| Diameter (mm) | 3.15±0.1 | 1.45±0.1 |
| Particle Density (kg/m ³) | 2750 | 2750 |
| Young's modulus (GPa) | 69 | 69 |
| Poisson ratio (ν) | 0.25 | 0.25 |
| Bulk density (kg/m ³) | 1680 | 1680 |

Table 2: DEM parameters: model silo

| Property | Glass beads |
|-----------------------------|-------------|
| Coefficient of restitution | 0.9 |
| Static friction p-w | 0.3 |
| Rolling friction p-w | 0.03 |
| Static friction p-p | 0.18 |
| Rolling friction p-p | 0.01 |
| Rayleigh time step (RTS), s | 6.7e-7 |
| Fixed time step, % | 10 |
| Data save interval, s | 0.005 |

The walls of the silo are made of Plexiglas which allows the measurement of the concentration and the velocity flows in the silo at the boundary. The particle trajectories in the silo are determined by means of image analysis through the front wall and the velocity fields are investigated by Particle Image Velocimetry (PIV) using geoPIV developed by White et al. [10]. PIV has been used extensively to study the velocity profiles of bulk solids; see [9,10]. The procedure is repeated whilst filling and emptying of the model silo.

The mesh used in the PIV study can be seen in Figure 1a and the velocity vectors at a time of 1s of discharge in Figure 1b. The concentration has been evaluated using image analysis. The analysis was performed with the same mesh as the one used for PIV and the Lacey segregation index calculated [1].

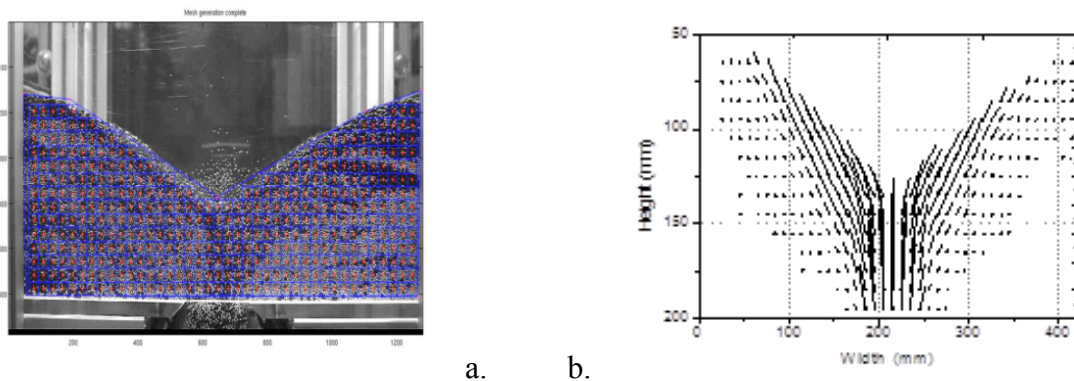


Figure 1: a. mesh of the silo used in PIV; b. PIV measurement of velocity vectors at 1s into discharge.

3.3 Ribbon blade mixer

Mixing behaviour was investigated in a laboratory size ribbon blade mixer. In order to validate DEM simulations an agitated mixer and real-life materials were chosen. Validation of simulation was performed by analysing mixing homogeneity over mixing time. This validation was carried out by analysis of samples, taken from the mixtures at different locations of the mixer.

The agitated mixer under investigation consists of a 10L mixing container with two helical mixing blades for active mixing, as shown in Figure 2a.

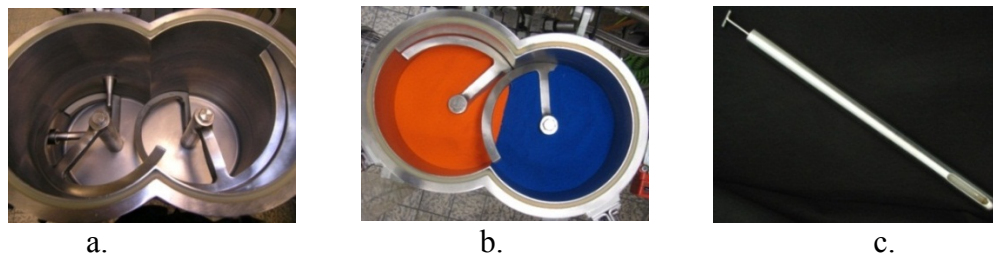


Figure 2: a. top view of the ribbon blade mixer; b. top view of the bladed mixer, filled with plastic granules; c. sampling thief with a slit length of 5 cm.

The material to be mixed is conveyed up along the blades and flows down near the shafts. The mixer was filled with plastic granules of two colours, but of similar size distributions in a volume ratio of 50:50 and up to a fill level of 70%, i.e. 7 L. The materials were loaded adjacent to each other, as shown in Figure 2b. Material properties may be found in Table 3.

Table 3: Material properties of plastic granules: mixer

| Property | Unit | Blue plastic granules |
|-----------------------------|-----------------|----------------------------|
| Size distribution, x_{10} | μm | 259 |
| Mean size, x_{50} | μm | 494 |
| Size distribution, x_{90} | μm | 994 |
| Sphericity | | 0.50 – 0.85 size dependent |
| Bulk density | kg/m^3 | 315 ± 6 |
| Property | Unit | Orange plastic granules |
| Size distribution, x_{10} | μm | 203 |
| Mean size, x_{50} | μm | 365 |
| Size distribution, x_{90} | μm | 629 |
| Sphericity | | 0.43 – 0.82 size dependent |
| Bulk density | kg/m^3 | 319 ± 5 |

Table 4: DEM input parameters: mixer

| Parameter | Value |
|---|---------------------|
| Young's modulus [Pa] | $2.5 \cdot 10^6$ |
| Poisson's ratio | 0.25 |
| Coefficient of restitution | 0.6 |
| Static friction coefficient (p-p) and (p-w)* | 0.5 |
| Rolling friction coefficient (p-p) and (p-w)* | 0.005 |
| Particle diameter [mm] | 5 |
| Particle density [kg/m^3] | 2200 |
| Rayleigh time [s] | $4.0 \cdot 10^{-4}$ |
| Time step [s] | $1 \cdot 10^{-5}$ |

* p-p represents particle- particle contacts, whereas p-w represents particle-wall contacts

In order to determine mixing homogeneity the mixture under investigation was sampled with a sample thief, shown in Figure 2c, the sampling procedure as presented by Simons et al. [45]. Samples were then analyzed by colour image analysis. With this analysis, fractions of each component could be calculated, from which mixing homogeneity could be determined.

DEM simulation input parameters were, as a first approach, non-calibrated, but defined with educated guesses, based on values from literature. These parameters are reported in Table 4. Sampling was done in a similar way as in the experimental results taking representative samples from 32 pre-defined mixer regions.

3.4 Fluidized beds

Including particle-air drag forces, segregation was also studied in a fluidized bed. The present work aims to calculate transport coefficients from carefully planned DEM simulations and a bi-disperse bed was modelled and studied to quantify segregation. The in house built open source coupled code LammmpsFOAM has been employed to study fluidisation [34]. Since DEM-CFD simulations for fluidisation of Geldart A and C powders [46] is cumbersome due to computational expense and small particle sizes (order of 100 μm) [47] large particles were simulated in the Geldart A and C regimes by addition of cohesive inter-particle forces in form of liquid bridge force model [48,49]. An evenly mixed bi-disperse bed is subjected to superficial inlet velocity greater than the minimum fluidisation velocity of “floatsam” particles (1.5 mm) but less than minimum fluidisation velocity of “jetsam” particles (2.5 mm). Simulations parameters are summarised in Table 5.

Table 5: Simulation parameters for the fluidized bed.

| Particle Properties (Glass beads) | | Floatsam | Jetsam |
|--|---------|-----------------------------------|----------------------|
| Particle size (mm) | | 1.5 | 2.5 |
| Density (kg/m^3) | | 2523 | 2526 |
| Number of particles | | 10178 | 10178 |
| Mass ratio | | 17% | 83% |
| Geldart Classification | | D | D |
| Experimental minimum fluidisation velocity | | 0.78 m/s | 1.25 m/s |
| Domain | | Discretization for fluid solver | |
| Width (x) | 0.15 m | NCellx | 15 |
| Depth (z) | 0.015 m | NCellz | 60 |
| Length (y) | 0.6 m | NCellz | 1 |
| Bed Height | 0.3 m | Nparticles/Cell | 200 |
| Initial bed porosity | 0.39 | Fluid time step | 1e-4 s |
| DEM Parameters | | Fluid parameters | |
| Stiffness k (N/m) | 2000 | Fluid density (kg/m^3) | 1.2 |
| Particle-particle coeff. of rest. | 0.97 | Dynamic viscosity (Pa.s) | 1.8e-5 |
| Friction coefficient | 0.15 | wall boundary conditions | Full slip |
| Particle-wall | | Particle time step | 1e-7 s |
| coeff. of restitution | 0.9 | Drag model | Beetstra et al. [42] |
| Friction coefficient | 0.10 | Averaging Kernel | Box-car |

Segregation in the fluidized bed is calculated according to the index mentioned in [11]. Segregation is apparent in the vertical direction; hence the index is defined in terms of averaged bed heights of floatsam and jetsam. Floatsam particles are fluidized with respect to bed, however drag forces are not large enough to counter the weight of heavier particles leading to segregation (heavier particles settle down). Segregation in fluidized bed has been

well studied before with respect to development of bi-disperse drag models, better closures and constitutive modelling [11,50,51]. However, segregation contributions from kinetic sieving and diffusion mechanisms have not been modelled in previous literature.

4. RESULTS AND DISCUSSION

4.1 State of mixing or segregation by mixing index

The state of segregation while discharging the silo can be seen in Figure 3, expressed as the Lacey mixing index over discharge time. The silo was filled with a mixture 50:50 in weight of both components as shown in Figure 4. During discharge the index increases indicating that the products remix while discharging. The Lacey index was measured for the same mixture using the QPM segregation tester obtaining a similar result.

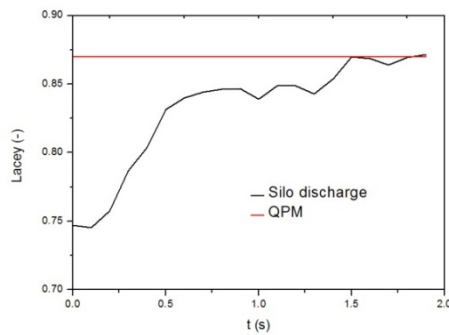


Figure 3: Lacey index of the content vs. time

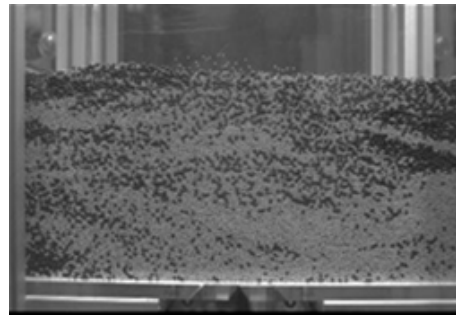


Figure 4: Initial state of the silo

The state of mixing in the ribbon blade mixer is shown in Figure 5, which compares the Lacey mixing index for simulation and experiments at 40 rpm. This mixing index, in both experiment (triangles) and simulation (cyan and red), rises relatively fast to unity for practically all fill heights. Experiment and simulation of the 70% fill height case were found in agreement, although input parameters for simulation were based on educated guesses. However, simulation results show a slight overprediction of mixing performance compared to experiments, probably caused by simplifications in simulation.

As shown in the insert in Figure 5, different fill heights in the mixer led to different mixing homogeneities achieved. Results indicated that at 70% fill height the highest mixing index was achieved. Similar results were found more pronounced for mixing experiments in the same mixer at 80 rpm (not shown here). This implies that with larger fill height better mixing performance is achieved, highlighting the importance of mixing in the axial, i.e. vertical direction. This complies with the fact that these types of ribbon blade mixers are normally operated at high fill levels [52].

The state of segregation for the bi-disperse fluidized bed case has been determined as well, indicating significant segregation within seconds.

For the examples above the state of segregation and mixing can be easily determined from experimental and DEM results for a mixture of different particles. Although the mixing index

may provide a good overall descriptor of segregation in a system at a given point in time, it provides no information on the spatial variation of the mixing and on the key mechanism(s) causing the segregation, which will be investigated next.

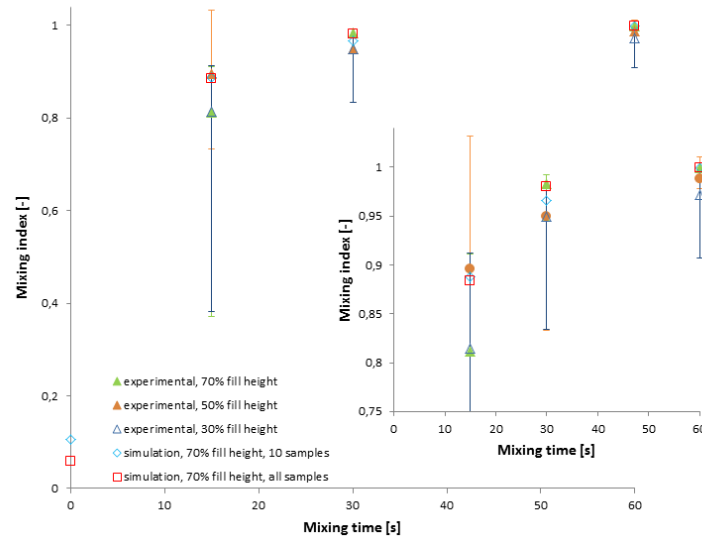


Figure 5: Simulated and experimental results for mixing index, calculated after Lacey [1] for ribbon blade mixer, mixing at 40 rpm. The insert shows the same results focusing on the results for 15s, 30s and 60s only. Error bars show 95% confidence intervals.

4.2 Diffusion and kinetic coefficients

The diffusion coefficients and the kinetic segregation coefficients as described in [24] have been calculated for the QPM tester, presuming a non-percolating material. Their variation with time is shown in Figure 6. The chute was gridded and the coefficients calculated for each particular volume. The coefficients in Figure 6 represent a statistical average of the coefficients obtained for the whole chute in the QPM. The coefficients are related to the coarser particles in the mixture in the case of kinetic segregation and for the smaller particles in the case of diffusion coefficient.

Figure 6b shows that the larger the size ratio between the two components of the mixture, the larger the diffusion coefficient and therefore the larger the remixing of the mixture. In the absence of diffusion the larger particles would rise up until two layers of particles are formed as stated by Gray and Ancy [53]. On the contrary, when increasing the size ratio of the bi-disperse mixture the kinetic segregation coefficient increases, leading to stronger segregation. In this manner the percolation mechanism can be explained.

For the fluidized bed, the diffusion and kinetic sieving coefficients were calculated from the fluctuating velocity components in the prevalent bed dynamics direction (along the gravity). Velocity and stress auto correlations were calculated for the total run of the simulation discarding the initial second. Coefficients were calculated from a representative bin in the middle half section of the bed. From this preliminary evaluation, relative

magnitudes of the two coefficients (Table 6) suggest that kinetic sieving dominates segregation mechanisms in this fluidized bed. Further investigations on homogenous and uniform fluidisation conditions are underway, to provide a fuller description of the phenomena involved.

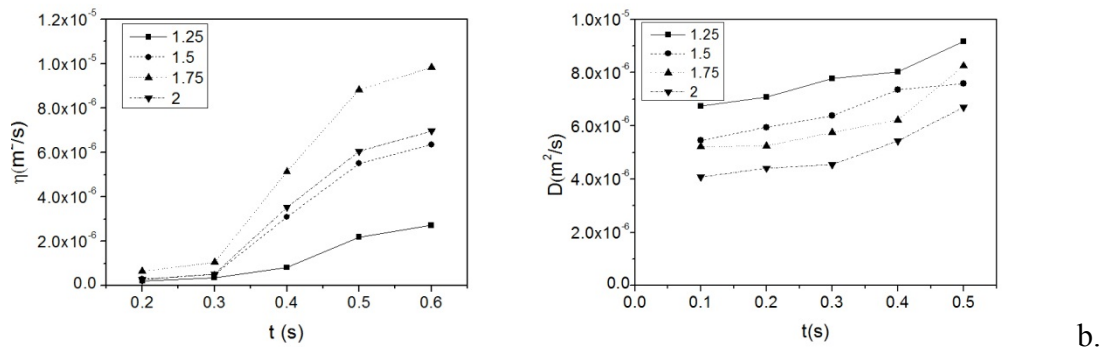


Figure 6: **a.** Average kinetic segregation coefficient with time for the QPM segregation tester; **b.** average diffusion coefficient with time for the QPM segregation tester

Table 6: Kinetic and Diffusion coefficients for the fluidized bed.

| | Kinetic Sieving Coefficient [m ² /s] | Diffusion Coefficient (V_y') [m ² /s] |
|--------|---|--|
| Fines | $2.5 \cdot 10^{-3}$ | $6.2608 \cdot 10^{-6}$ |
| Coarse | $5.4 \cdot 10^{-3}$ | $4.2812 \cdot 10^{-5}$ |

Both applications lead to a significant difference between the kinetic sieving and the diffusion based segregation coefficients, especially in the case of the fluidized bed. These highlight the importance of kinetic sieving and hence the shear dependent segregation in both applications. This is especially true when percolation contribution is rather weak or negligible. In the case when percolation becomes more prominent, the diffusion mechanism is expected to become more significant, due to the dynamics of the system. It is therefore reasonable to suggest here that the particle systems studied are essentially non-percolating mixtures where segregation is driven by kinetic sieving and local shear gradients in flow.

5. CONCLUSIONS AND OUTLOOK

- The state of, propensity towards and causes of segregation and mixing have been analyzed for three industrial applications involving granular mixtures.
- Lacey's mixing index is particularly appropriate for quantifying segregation/mixing in non-percolating mixtures where the shear gradients induced by mixer action drives the mixing process. When trying to mix percolating mixtures with higher particle size ratios, it will then be necessary to use a composite index made up of kinetically-driven mixing and gravity-driven percolation to quantify the individual but opposite mechanisms occurring in the mixer.

- The mechanisms of segregation have been evaluated and quantified for the silo discharge and the bi-disperse fluidized bed using the segregation model. The most significant outcome is the orders of magnitude difference between the kinetic sieving and the diffusion based segregation coefficients. These highlight the importance of kinetic sieving and hence the shear dependent segregation in both applications. This is especially true when percolation contribution is rather weak or negligible. Diffusion becomes more significant when percolation starts to contribute. It is therefore reasonable to suggest that the particle systems looked at are essentially non-percolating mixtures where segregation is driven by kinetic sieving and local shear gradients in flow.
- It is encouraging to see that identical treatment of experimental and simulation results obtained in chutes, silos, helical ribbon mixers and fluidized beds could be used to cross-validate within the same modeling framework for segregation and mixing processes in free-flowing, bi-disperse materials. This is believed to be a very encouraging outcome upon which further work could be built to model mixing and segregation in more poly-disperse and cohesive materials.
- The quantification of segregation mechanisms paves the way for scaling-up to continuum models for industrial applications of silos, mixers and fluidized beds, saving extensive large-scale experiments and lengthy DEM(-CFD) calculations.

ACKNOWLEDGEMENTS

The authors wish to thank the EU Marie Curie actions ITN. The funding for the project (Project No. ITN-238577) is gratefully acknowledged.



REFERENCES

- [1] Lacey, P.M.C., *Journal of Applied Chemistry* (1954) **4(5)**: 257–268
- [2] Carley-Macaulay, K.W. and Donald, M.B., *Chemical Engineering Science* (1962) **17**: 493-506
- [3] Müller, W. and Rumpf, H., *Chemie Ingenieur Technik* (1967) **39**: 365 – 373
- [4] Yeung, C.C. and Hersey, J.A., *Powder Technology* (1979) **22**: 127 - 131
- [5] Kehlenbeck, V. and Sommer, K., *Powder handling and processing* (2003) **15(5)**: 318-327
- [6] McGlinchey, D., *Powder Technology* (2004) **145**: 106 – 112
- [7] Conway, S.L., Lekhal, A., Khinast, J.G. and Glasser, B.J., *Chemical Engineering Science* (2005) **60**: 7091-7107
- [8] Remy, B., Canty, T.M., Khinast, J.G. and Glasser, B.J., *Chemical Engineering Science* (2010) **65**: 4557-4571
- [9] Ostendorf, M. and Schwedes, J., *Powder Technology* (2005) **158**: 69-75

- [10] White, D.J., Take, W.A. and Bolton, M.D., *Geotechnique*, (2003) **53(7)**: 619-631
- [11] Goldschmidt, M.J.V., Link, J.M., Mellema, S. and Kuipers, J.A.M., *Powder Technology* (2003) **138(2)**: 135–159
- [12] Stewart, R.L., Bridgwater, J. and Parker, D.J., *Chemical Engineering Science* (2001) **56**: 4257-4271
- [13] Shepperson, J., Seville, J.P.K., Greenwood, R.W. and Knight, P.C., *7th Bulk Materials Storage, Handling and Transportation Conference*, Newcastle, New South Wales, Australia, October 2001, Vol. 1, 151 -161
- [14] Jones, J.R., Parker, D.J. and Bridgwater, J., *Powder Technology* (2007) **178**: 73-86
- [15] Hassanpour, A., Tan, H., Bayly, A., Gopalkrishnan, P., Ng, B. and Ghadiri, M., *Powder Technology* (2011) **206**: 189-194
- [16] Zhou, Y.C., Yu, A.B., Stewart, R.L. and Bridgwater, J., *Chemical Engineering Science* (2004) **59**: 1343-1364
- [17] Remy, B., Khinast, J.G. and Glasser, B.J., *AIChE Journal* (2009) **55(8)**: 2035-2048
- [18] Chandratilleke, G.R., Zhou, Y.C, Yu, A.B. and Bridgwater, J., *Ind. Eng. Chem. Res.* (2010) **49**: 5467-5478
- [19] Fan, L.T., and Wang, R.H., *Powder Technology* (1975) **11**: 27 – 32
- [20] Poux, M., Fayolle, P., Bertrand, J., Bridoux, D. and Bousquet, J., *Powder Technology* (1991) **68**: 213-234
- [21] Baxter, J., Gröger, T., Abou-Chakra, H., Tüzün, U., Christakis, N., Patel, M.K. and Cross, M., “Micro-mechanical parameterisations for Continuum Modelling of Granular Material Using the Discrete Element Method; presentation at *5th World Congress on Computational Mechanics (WCCM)*, Vienna, Austria, July 7-12, 2002
- [22] Christakis, N., Chapelle, P., Strusevich, N., Bridle, I., Baxter, J., Patel, M.K., Cross, M., Tüzün, U., Reed, A.R. and Bradley, M.S.A., *Advanced Powder Technology* (2006) **17**: 641-662
- [23] Christakis, N., Patel, M.K., Cross, M. and Tüzün, U., “On the Modelling of Complex Systems-Methodologies and Applications,” in *9th International Symposium on Distributed Computing and Applications to Business Engineering and Science (DCABES)*, Hong Kong, China, August 2010, 40–45
- [24] Christakis, N., Patel, M.K., Cross, M., Baxter, J., Abou-Chakra, H. and Tüzün, U., *International journal for numerical methods in fluids*, (2002) **40(1-2)**: 281–291
- [25] Zigan, S., Thorpe, R.B., Tüzün, U. and Enstad, G.G., *Particle & Particle Systems Characterization* (2007) **24(2)**: 124–135
- [26] Zigan, S., Thorpe, R.B., Tüzün, U., Enstad, G.G. and Battistin, F., *Powder Technology* (2008) **183**: 133-145
- [27] McQuarrie, D.A., *Statistical mechanics* Harper and Row, New York, 1976
- [28] Zwanzig, R., *Annual Review of Physical Chemistry*, (1965) **16(1)**: 67-102
- [29] Valverde, J., Castellanos, A. and Sanchez Quintanilla, M.A., *Physical Review Letters* (2001) **86(14)**: 3020-3023
- [30] Natarajan, V.V.R., Hunt, M.L. and Taylor, E.D., *Journal of Fluid Mechanics* (1995) **304**: 1-25

- [31] Zivkovic, V., Biggs, M.J., Glass, D.H. and Xie, L., *Advanced Powder Technology* (2009) **20(3)**: 227–233
- [32] Wildman, R.D., Huntley, J.M. and Hansen, J.-P., *Physical Review E* (1999) **60(6)**: 7066–7075
- [33] Kloss, C., Goniva, C., Hager, A., Amberger, S. and Pirker, S., *Progress in Computational Fluid Dynamics, an International Journal* (2012) **12(2)**: 140–152
- [34] Xiao, H. and Sun, J., *Communications in Computational Physics* (2011) **9**: 297–323
- [35] Cundall, P.A. and Strack, O.D.L., *Geotechnique* (1979) **29(1)**: 47–65
- [36] Tsuji, Y., Tanaka, T. and Ishida, T., *Powder Technology* (1992) **71**: 239–250
- [37] Ai, J., Chen, J.-F., Rotter, J.M. and Ooi, J.Y., *Powder Technology* (2011) **206**: 269–282
- [38] Sun, J., Battaglia, F. and Subramaniam, S., *Journal of Fluid Engineering* (2007) **129**: 1394–1403
- [39] Quintanilla, M., Castellanos, A. and Valverde, J., *Physical Review E* (2001) **64(3)**: 031301
- [40] Jackson, R., *Chemical Engineering Science* (1997) **52(15)**: 2457–2469
- [41] Anderson, T.B. and Jackson, R., *Industrial & Engineering Chemistry Fundamentals* (1967) **6(4)**: 527–539
- [42] Beetstra, R., Hoef, M. A. van der and Kuipers, J.A.M., *AIChE Journal* (2007), **53(2)**: 489–501
- [43] Bridle, I., Bradley, M., Reed, A., Abou-Chakra, H., Tüzün, U. and Farnish, R. “Development of a test instrument to measure the segregation propensity of bulk materials”, in *8th Int. Conf. on Bulk Materials Storage Handling and Transportation*, Wollongong, Australia 2004
- [44] Combarros, M., Feise, H.J., Zetzener, H. and Kwade, A., “Segregation of particulate solids: Experiments and DEM simulations” *Particuology* (2013) (In press)
- [45] Simons, T.A.H., Bensmann, S., Zetzener, H., Schilling, M., Kleine-Jäger, F., Feise, H.J. and Kwade, A., “Experiments and simulations of granular flow in a helical ribbon blade mixer”, in *7th International Conference for Conveying and Handling of Particulate Solids – CHoPS*, September 2012, Friedrichshafen, Germany
- [46] Geldart, D., *Powder technology* (1973) **7(5)**: 285–292
- [47] Pandit, J.K., Wang, X.S. and Rhodes, M.J., *Powder Technology* (2005) **160(1)**: 7–14
- [48] Rhodes, M.J., Wang, X.S., Nguyen, M., Stewart, P. and Li, K., *Chemical Engineering Science* (2001) **56(14)**: 4433–4438
- [49] Mikami, T., Kamiya, H. and Horio, M., *Chemical Engineering Science* (1998) **53(10)**: 1927–1940
- [50] Feng Y.Q. and Yu, A.B., *Industrial & Engineering Chemistry Research* (2010) **49(7)**: 3459–3468
- [51] Di Maio, F.P., Di Renzo, A. and Vivacqua, V., *Powder Technology* (2012) **226**: 180–188
- [52] Cooker, B. and Nedderman, R.M., *Powder Technology* (1987) **50**: 1–13
- [53] Gray, J.M.N.T. and Ancy, C., *Journal of Fluid Mechanics* (2011) **678**: 535–588